Dedicated to my beloved Father

Sri. Deepak Kumar Das

Baba your unconditional support and faith is the ultimate moral boosting power that helped me throughout my journey

You are the supporting pillar in my life

Thank you for all

Declaration

I, Dipayan Das hereby declare that the work embodied in my Ph.D thesis entitled "APPLICATION OF NANO SILVER AND SILVER IONS IN PRESERVATION OF MULBERRY LEAVES AND THEIR UTILIZATION IN SILKWORM REARING SYSTEM" *has been carried out by me under the supervision of* ***Dr. Palash Mandal*** *Department of Botany, University of North Bengal for the award of the degree of Doctor of Philosophy in Botany. I also declare that, this thesis or any part thereof has not been submitted for any other degree/diploma either to this or other University.*

Dipayan Das

[Dipayan Das]

Date: 27.09.2021

Place: Department of Botany,
University of North Bengal
Siliguri- 734013

ENLIGHTMENT
TO PERFECTION

UNIVERSITY OF NORTH BENGAL

ACCREDITED BY NAAC WITH GRADE A

Department of Botany

Raja Rammohunpur, Siliguri – 734013, West Bengal, India

Visit us at:
www.nbu.ac.in

Dr. Palash Mandal; Ph: +91- 9434886123; E-mail: pmandalbotppprl@nbu.ac.in

TO WHOM IT MAY CONCERN

This is to certify that the thesis entitled, **"APPLICATION OF NANO SILVER AND SILVER IONS IN PRESERVATION OF MULBERRY LEAVES AND THEIR UTILIZATION IN SILKWORM REARING SYSTEM"** *submitted by Mr. Dipayan Das for the award of the degree of Doctor of Philosophy in Botany is based on the results of experiments carried out by him. He has worked under my supervision at Department of Botany, University of North Bengal. I am forwarding his thesis for the Ph.D. degree (Science) in Botany of the University of North Bengal. He has fulfilled all requirements according to the rules of the University of North Bengal regarding the works embodied in his thesis. This thesis or any part thereof has not been submitted for any other degree/Diploma either to this or other University.*

He bears good moral character and I wish him best for his future.

Date: 27th Sept., 2021

Place: Department of Botany,
University of North Bengal
Siliguri- 734013

Palash Mandal

(Dr. Palash Mandal)

Supervisor

Dr. PALASH MANDAL
Dept. of Botany
University of North Bengal

Curiginal

Document Information

Analyzed document	Dipayan Das_Botany.pdf (D112679864)
Submitted	9/16/2021 8:40:00 AM
Submitted by	University of North Bengal
Submitter email	nbuplg@nbu.ac.in
Similarity	1%
Analysis address	nbuplg.nbu@analysis.urkund.com

Sources included in the report

W	URL: https://www.ncbi.nlm.nih.gov/pmc/articles/PMC166603/ Fetched: 9/17/2021 12:10:00 AM	2
W	URL: http://www.maths.surrey.ac.uk/hosted-sites/R.Knott/Fibonacci/cfINTRO.html Fetched: 9/17/2021 12:10:00 AM	2
W	URL: https://link.springer.com/content/pdf/bbm%253A978-0-8176-8286-6%252F1.pdf Fetched: 9/17/2021 12:10:00 AM	1
W	URL: https://www.missouristate.edu/Assets/assessment/annual_report_CNAS_2016_Geography_Geology_Planning.pdf Fetched: 9/17/2021 12:10:00 AM	2
W	URL: https://www.arabidopsis.org/servlets/TairObject%253Ftype%253Dlocus%2526name%253DAt2g01330 Fetched: 9/17/2021 12:10:00 AM	8
W	URL: https://www.uniprot.org/uniprot/Q9M2C4 Fetched: 9/17/2021 12:10:00 AM	5
W	URL: https://www.uniprot.org/docs/arath.txt Fetched: 9/17/2021 12:10:00 AM	35
W	URL: https://www.ncbi.nlm.nih.gov/gene/825312 Fetched: 9/17/2021 12:10:00 AM	5

Dipayan Das
Department of Botany
University of North Bengal

Dr. Palash Mandal
(Supervisor)
Department of Botany
University of North Bengal

Dr. PALASH MANDAL
Dept. of Botany
University of North Bengal

Acknowledgement

At the virtue of completing my Ph.D work, when I look back, I find that in the background continuous help and support of lot of faces persist, whom I like to recognize as moral boosting power in completing my dissertation work.

Firstly, I would like to explicit my cordial gratitude to my supervisor Dr. Palash Mandal for his continuous support and motivation in completing my Ph.D dissertation and related research works. His guidance and assistance helped me throughout the period of research and writing of this thesis. Whenever I faced challenges, he was next to me and sometime one step forward in tackling the problems. From the depth of my heart I would like to state that I could not have imagined a better mentor than him as Ph.D supervisor.

I would like to express my heartiest gratitude to, Head of the Department of Botany Dr. Manoranjan Chowdhury, University of North Bengal for allowing me to access different facilities of the Department, alongside his continuous support and motivation.

I would also like to express my warm-hearted gratitude to all the faculty members of Department of Botany, University of North Bengal namely Prof. Aniruddha Saha, Prof. Arnab Sen, Prof. Subhas Chandra Roy, Dr. Jnan Bikash Bhandari, Dr. Piyush Mathur, Dr. Swarnendu Roy for their support and motivation.

I would also like to extend my thanks to all the non-teaching staff of the Department of Botany, University of North Bengal for their kind support time to time.

I would like to thank Late (Dr.) Madhur Pramanik, whom I recognize as an Acharya, helped me to learn the basic of bioscience in my post-school days, consolidating my base towards this branch of science.

I am extending my regards to Dr. Kailash Choudhary who helped me to consolidate my base in higher order biology which eventually helped me to summarize the outcome of my research work.

My work would have been incomplete without constant help and assistance from Directorate of Textiles (Sericulture), Govt. of West Bengal, Matigara Sericulture Complex and Naxalbari Sericulture Complex. I would like to convey my heartiest thanks to Mr. Manab Bhowmick and all other members of sericulture department for extending their helping hand time to time in my entire research tenure. I am extremely thankful to Mr. Saurabh Majumdar, Scientist-D, RSTRS, Central Silk Board for helping me by analyzing the cocoons for post cocoon parameters.

I would also like to thank SAIF (IIT Bombay), SAIF (Cochin University of Science and Technology) and USIC (University of North Bengal) for assisting me while conducting various instrumental analyses.

I am thankful to University Grants Commission for providing me the research fellowship under UGC-NET JRF and UGC-NET SRF scheme.

Working in a wet-lab, I realized that the ultimate thing was team work without which one cannot complete the dissertation work. I am extremely thankful to my laboratory seniors from whom I have learned the initial steps in research namely Ms. Arunika Subba, Dr. Sumira Mukhia, Dr. Saran Kumar Gupta, Mr. Sujoy Sen and Mr. Priyankar Roy. I express my gratitude towards my younger brothers and sisters in my laboratory namely Md. Salman Haydar, Ms. Divya Chauhan, Mr. Kushankur Sarkar, Mr. Swarup Singha Roy, Ms. Deboshmita Ghosh and Ms. Surovi Ghosh for extending their helping hands.

I convey my special thanks to Dr. Prasanjit Chakraborty, Former Research Scholar, Department of Botany, University of North Bengal; Dr. Raja Ghosh, Former Research Scholar, Department of Chemistry, University of North Bengal; Mr. Subhrajyoti Bagchi, State Aided College Teacher, Department of Computer Science and Applications, Malda College and Mr. Arindam Ghosh, Researcher, Institute of Biomedicine, University of Eastern Finland for extending their unconditional help.

I express my gratitude, love and regards to all of my friends and friend like seniors namely Mr. Indrajit Singha, Ms. Tanushree Sarkar, Mr. Asit Ray, Ms. Puja Sashankar, Dr. Krishna Jaiswal, Mr. Ujjal Roy, Mr. Buddhadev Sarkar, Mr. Shahid Sarkar, Mr. Subhro Sarkar, Dr. Sibhu Das and Mr. Pankaj Shil who stood behind me, specifically in my difficult time throughout my journey. I would like to emphasize the unconditional extended help of Mr. Indrajit Singha (Indra) who provided me space to sleep and food to eat on numerous occasions during my research tenure when I worked night long in my laboratory.

I would like to thank Dr. Payel Paul for her moral support and valuable suggestions throughout my research tenure, especially during early days when the path was bit difficult to walk alone. Being a true friend, her blind faith in me has motivated me to take challenges in life, some of them has really paid off.

Last but not the least, I would like to express my gratitude towards my parents (Sri. Deepak Kumar Das and Smt. Debjani Das) whose continuous support, love and blessings has encouraged me to extend my carrier in the field of science and research. I would also like to express my love and affection towards my brother (Mr. Debraj Das) who stood behind me all the times. I am also thankful to my in-laws (Sri. Debabrata Paul and Smt. Mridula Paul) for their support and blessings. At the end I would like to recall the memories of my grandparents [Late (Sri.) Bhupendra Nath Das, Late (Smt.) Santi Bala Das, Late (Sri) Ananda Kishor Ghosh and Late (Smt.) Namita Ghosh], the persons whose morality towards life has influenced me the most from my childhood.

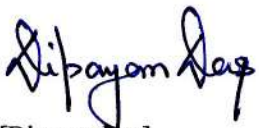

[Dipayan Das] September, 2021

Department of Botany
University of North Bengal

List of Tables

List of Figures

Fig. 18: Illustration of venation pattern in mulberry cultivars under study (**a**) V1and (**b**) Guangdong

Fig. 19: Light microscopic plates displaying nature of glandular trichomes in all the cultivars of mulberry under study *viz.*S1635 (**a**), TR10 (**b**), S1 (**c**), BC259 (**d**), V1 (**e**) and Guangdong (**f**)

Fig. 20: Scanning Electron Microscopic plates displaying nature of glandular trichomes in all the cultivars of mulberry under study *viz.*S1635 (**a**), TR10 (**b**), S1 (**c**), BC259 (**d**), V1 (**e**) and Guangdong (**f**)

Fig. 21: Light microscopic plates displaying nature of non-glandular trichomes in all the cultivars of mulberry under study *viz.*S1635 (**a**), TR10 (**b**), S1 (**c**), BC259 (**d**), V1 (**e**) and Guangdong (**f**)

Fig. 22: Scanning Electron Microscopic plates displaying nature of non-glandular trichomes in all the cultivars of mulberry under study *viz.*S1635 (**a**), TR10 (**b**), S1 (**c**), BC259 (**d**), V1 (**e**) and Guangdong (**f**)

Fig. 23: Light microscopic plates displaying nature of idioblast in all the cultivars of mulberry under study *viz.*S1635 (**a**), TR10 (**b**), S1 (**c**), BC259 (**d**), V1 (**e**) and Guangdong (**f**)

Fig. 24: Pearson correlation coefficient matrix of different micro- and macro-morphological traits under study

Fig. 25: Principal component analysis of six mulberry cultivars and different micro- and macro-morphological traits under study (Yellow dots represents mulberry cultivars, while green, orange, red, violet and blue dots represents laminar, trichome, stomatal, venation and idioblast attributes respectively)

Fig. 26: Dendrogram representing similarity clusters of six mulberry genotype under study with respect to overall parameters

Fig. 27: Pictorial view representing physical condition of mulberry leaves preserved for 7 days in nine different preservative solutions. (**a-b**) 1D and 7D distilled water preserved leaves; (**c-f**) 0.1, 1, 5, 10 mM indole acetic acid; (**g-j**) 10^{-6}, 10^{-5}, 10^{-4}, 10^{-3} M kinitin; (**k-m**) 0.05 mM, 10^{-4}, 10^{-3}, 10^{-2} M benzyl adenine; (**o-r**) 0.05, 0.1, 0.5, 1 mM gibberellic acid; (**s-v**) 0.1, 0.5, 1, 2 mM salicylic acid; (**w-z**) 200, 400, 600, 800 ppm putricine; (**aa-ad**) 0.05, 0.01, 0.1, 1 mM sodium nitroprusside; (**ae-ah**) 10, 50, 100, 150 ppm silver nitrate; (**ai-al**) 50, 100, 200, 300 µM silver thiosulphate preserved leaves respectively

Fig. 28: Effect of preservation on total chlorophyll content of mulberry leaves preserved with different preservative solutions. The effect of preservation was compared with respect

Fig. 81: Long term stability assessment as a function of plasmon peak deformation through UV-Vis spectrophotometer of silver nanoparticles phytosynthesized by varying concentration of silver nitrate, (**A-F**) spectral reading at an interval of 10, 20, 30, 40, 50, 60 days respectively

Fig. 82: Long term stability assessment as a function of plasmon peak deformation through UV-Vis spectrophotometer of silver nanoparticles phytosynthesized by varying volume of plant extract, (**A-F**) spectral reading at an interval of 10, 20, 30, 40, 50, 60 days respectively

Fig. 83: Long term stability assessment as a function of plasmon peak deformation through UV-Vis spectrophotometer of silver nanoparticles phytosynthesized at different proportion of plant extract to silver nitrate, (**A-F**) spectral reading at an interval of 10, 20, 30, 40, 50, 60 days respectively

Fig. 84: Long term stability assessment as a function of plasmon peak deformation through UV-Vis spectrophotometer of silver nanoparticles phytosynthesized by varying pH of plant extract, (**A-F**) spectral reading at an interval of 10, 20, 30, 40, 50, 60 days respectively

Fig. 85: Long term stability assessment as a function of plasmon peak deformation through UV-Vis spectrophotometer of phytosynthesized silver nanoparticles at different temperature range, (**A-F**) spectral reading at an interval of 10, 20, 30, 40, 50, 60 days respectively

Fig. 86: Physical condition of mulberry leaves preserved in nanosilver solution phytosynthesized at different concentration of silver nitrate

Fig. 87: Physical condition of mulberry leaves preserved in nanosilver solution phytosynthesized with mulberry leaf extract adjusted to pH 2, 5, 7, 9 and 12

Fig. 88: Physical condition of mulberry leaves preserved in nanosilver solution phytosynthesized at different temperature range *viz.* 0, 10, 25, 50 and 80˚C

Fig. 89: Pictorial view representing physical condition of S1 genotype mulberry leaves preserved for 7 days in three different dilutions of 10^{-3} M silver nanoparticles *viz.* 10x (**A**), 20x (**B**) and 40x (**C**)

Fig. 90: Physical changes in mulberry leaves with increase in days of preservation (left to right: day 1 to day 7). Leaves were preserved in (**a**) Control (distilled water); (**b**) Nanosilver; (**c**) Silver nitrate solution

Fig. 91: Effect of preservation of S1 genotype of mulberry leaves with distilled water, nanosilver and silver nitrate on (**A**) total chlorophyll, (**B**) total protein, (**C,D**) total and reducing sugar and (**E**) proline content. Effect of preservative solutions on mulberry leaves

was observed at regular interval of 0D, 1D, 4D, 6D and 7D. The results were expressed as Mean ± SDEV, n= 3

Fig. 92: Effect of preservation of S1 genotype of mulberry leaves with distilled water, nanosilver and silver nitrate on (**A**) hydrogen peroxide, (**B**) superoxide and (**C**) malondialdehyde content. Effect of preservative solutions on stress content of mulberry leaves was observed at regular interval of 0D, 1D, 4D, 6D and 7D. The results were expressed as Mean ± SDEV, n= 3

Fig. 93: Two tailed Pearson correlation representing interrelationship among the post-preservative quality detecting parameters and rearing parameters

Fig. 94: Effect of preservation of S1 genotype of mulberry leaves with distilled water, nanosilver and silver nitrate on (**A**) diphenyl-1-picrylhydrazyl, (**B**) 2,2-azino-bis 3-ethylbenzthiazoline-6-sulphonic acid, (**C**) superoxide, (**D**) nitric oxide and (**E**) metal chelating activity. Effect of preservative solutions on antioxidant activity of mulberry leaves was observed at regular interval of 0D, 1D, 4D, 6D and 7D. Smaller the IC50 value more was the antioxidant activity. The results were expressed as Mean ± SDEV, n= 3

Fig. 95: Effect of preservation of S1 genotype of mulberry leaves with distilled water, nanosilver and silver nitrate on (**A**) superoxide dismutase, (**B**) catalase, (**C**) ascorbate peroxidase, (**D**) glutathione S-transferase, (**E**) glutathione peroxidase and (**F**) glutathione disulfide reductase content. Effect of preservative solutions on antioxidant enzymatic activity of mulberry leaves was observed at regular interval of 0D, 1D, 4D, 6D and 7D. Larger the content, greater was the defensive activity, less was the stress accumulation. The results were expressed as Mean ± SDEV, n= 3

Fig. 96: Effect of preservation of S1 genotype of mulberry leaves with distilled water, nanosilver and silver nitrate on (**A**) carotenoids, (**B**) ascorbic acid and (**C**) total glutathione content. Effect of preservative solutions on non-enzymatic antioxidant activity of mulberry leaves was observed at regular interval of 0D, 1D, 4D, 6D and 7D. The results were expressed as Mean ± SDEV, n= 3

Fig. 97: Effect of preservation of S1 genotype of mulberry leaves with distilled water, nanosilver and silver nitrate on (**A**) total phenol, (**B**) ortho-dihydric phenol and (**C**) flavonoid content. Effect of preservative solutions on secondary metabolite content of mulberry leaves was observed at regular interval of 0D, 1D, 4D, 6D and 7D. The results were expressed as Mean ± SDEV, n= 3

Fig. 98: SDS gel portrait and scanned image of protein bands in nanosilver preserved mulberry leaves (1 to 7 denotes Day 1 to Day 7)

Fig. 112: On-gel (**a**) image and (**b**) scanned photograph showcasing catalase activity of (**1-2**) fresh leaves and 7 days preserved mulberry leaves in (**3-4**) distilled water, (**5-6**) nanosilver and (**7-8**) silver nitrate solution

Fig. 113: Graphical representation depicting relative density of catalase activity of fresh mulberry leaves and 7 days preserved mulberry leaves in distilled water, nanosilver and silver nitrate solution. Numerical (1, 2, 3,...) at the top of graphical bars denotes band numbers

Fig. 114: On-gel (**a**) image and (**b**) scanned photograph showcasing peroxidase activity of (**1-2**) fresh leaves and 7 days preserved mulberry leaves in (**3-4**) distilled water, (**5-6**) nanosilver and (**7-8**) silver nitrate solution

Fig. 115: Graphical representation depicting relative density of peroxidase activity of fresh mulberry leaves and 7 days preserved mulberry leaves in distilled water, nanosilver and silver nitrate solution. Numerical (1, 2, 3,...) at the top of graphical bars denotes band numbers

Fig. 116: Nutrient agar plates representing antimicrobial activity of preservative solutions at different days of preservation: **IA-IG** CFU count of distilled water used as preservative from day 1 to day 7; **IIA-IIG** CFU count of silver nitrate solution used as preservative from day 1 to day 7; **IIIA-IIIG** CFU count of nanosilver solution used as preservative from day 1 to day 7

Fig. 117: Pictorial view representing physical condition of S1, S1635, TR10, BC259 and Guangdung genotype mulberry leaves preserved for 7 days in preservative solutions: **I** fresh leaves; **II**, **III** and **IV** represents 7 day preserved leaves in nanosilver, silver nitrate and distilled water respectively

Fig. 118: Total chlorophyll content in leaves of five mulberry cultivars, preserved with 6 ppm nanosilver solution (**A**), 6 ppm silver nitrate solution (**B**) and distilled water (**C**) for seven days in comparison to initial day

Fig. 119: Total protein content in leaves of five mulberry cultivars, preserved with 6 ppm nanosilver solution (**A**), 6 ppm silver nitrate solution (**B**) and distilled water (**C**) for seven days in comparison to initial day

Fig. 120: Total sugar content in leaves of five mulberry cultivars, preserved with 6 ppm nanosilver solution (**A**), 6 ppm silver nitrate solution (**B**) and distilled water (**C**) for seven days in comparison to initial day

Fig. 121: Transverse section of the petioles of mulberry leaf under light (**A**) and electron (**B**) microscope indicating different layers from outside to inside as star mark: trichome, CU:

cuticle, EP: epidermis, CO: collenchyma, P: parenchyma, ID: idioblast, PH: phloem, MX: metaxylem, PX: protoxylem, PI: pith

Fig. 122: Histochemical identification of protein components in xylem occlusions by Bradford reagent in petiole of mulberry leaves: (**A**) fresh leaves, (**B**) 7 day distilled water preserved leaves; (**C**) 7 day nanosilver preserved leaves, (**D**) 7 day silver nitrate preserved leaves; **I – V** represents S1, S1635, TR10, BC259 and Guangdung genotype of mulberry leaves used for preservation respectively

Fig. 123: Histochemical identification of lignins in xylem occlusions by Azure B in petiole of mulberry leaves: (**A**) fresh leaves, (**B**) 7 day distilled water preserved leaves; (**C**) 7 day nanosilver preserved leaves, (**D**) 7 day silver nitrate preserved leaves; **I – V** represents S1, S1635, TR10, BC259 and Guangdung genotype of mulberry leaves used for preservation respectively

Fig. 124: Histochemical identification of lignins in xylem occlusions by Phloroglucinol–HCl in petiole of mulberry leaves: (**A**) fresh leaves, (**B**) 7 day distilled water preserved leaves; (**C**) 7 day nanosilver preserved leaves, (**D**) 7 day silver nitrate preserved leaves; **I – V** represents S1, S1635, TR10, BC259 and Guangdung genotype of mulberry leaves used for preservation respectively

Fig. 125: Histochemical identification of suberins in xylem occlusions by Sudan IV in petiole of mulberry leaves: (**A**) fresh leaves, (**B**) 7 day distilled water preserved leaves; (**C**) 7 day nanosilver preserved leaves, (**D**) 7 day silver nitrate preserved leaves; **I – V** represents S1, S1635, TR10, BC259 and Guangdung genotype of mulberry leaves used for preservation respectively

Fig. 126: Scanning electron micrograph showing xylem occlusions in petiole of mulberry leaves: (**A**) fresh leaves, (**B**) 7 day distilled water preserved leaves; (**C**) 7 day nanosilver preserved leaves, (**D**) 7 day silver nitrate preserved leaves; **I – V** represents S1, S1635, TR10, BC259 and Guangdung genotype of mulberry leaves used for preservation respectively

Fig. 127: Histochemical detection of hydrogen peroxide localization by potassium iodide and starch solution in petiole of mulberry leaves: (**A**) fresh leaves, (**B**) 7 day distilled water preserved leaves; (**C**) 7 day nanosilver preserved leaves, (**D**) 7 day silver nitrate preserved leaves; **I – V** represents S1, S1635, TR10, BC259 and Guangdung genotype of mulberry leaves used for preservation respectively

Fig. 128: Histochemical detection of plasma membrane integrity by Evan's blue in petiole of mulberry leaves: (**A**) fresh leaves, (**B**) 7 day distilled water preserved leaves; (**C**) 7 day

Fig. 153: STRING second round analysis of selected up-regulated unigenes those are found to be significantly enriched from round one GO analysis. STRING network contains 71 node connected by 298 edges having PPI enrichment of p< 1.0e-16

Fig. 154: STRING second round analysis of selected down-regulated unigenes those are found to be significantly enriched from round one GO analysis. STRING network contains 82 node connected by 216 edges having PPI enrichment of p< 1.0e-16

Fig. 155: Topological networking of STRING (second round) generated up-regulated gene interaction data using cytoscape platform. Cytoscape connected 65 nodes with network density and homogeneity of 0.143 and 0.613 respectively, with characteristic path length of 2.480 and average number of neighbours of 9.169

Fig. 156: Topological networking of STRING (second round) generated down-regulated gene interaction data using cytoscape platform. Cytoscape connected 74 nodes with network density and homogeneity of 0.080 and 0.690 respectively, with characteristic path length of 2.785 and average number of neighbours of 5.835

Fig. 157: Expression profile of topologically selected top up-regulated genes

Fig. 158: Functional sub-networking of highly interconnected nodes (up-regulated genes) using MCODE. Networks were built considering note density and node score cut-off value of 0.1, 0.2 respectively, with kappa-core value of 2

Fig. 159: Expression profile of topologically selected top down-regulated genes

Fig. 160: Functional sub-networking of highly interconnected nodes (down-regulated genes) using MCODE. Networks were built considering note density and node score cut-off value of 0.1, 0.2 respectively, with kappa-core value of 2

Fig. 161: Gene ontological enrichment analysis of topologically selected up-regulated genes based on biological process using BiNGO considering *Arabidopsis* as model organism. Hypergeometric test was conducted, considering p-value cut off ≤ 0.05. Size of the node was proportional to the number of gene (transcripts) present under a particular nodal category. Node colour shades were according to the significance level where white represents no significant differences, yellow and green colour shade represents significance level at p = 0.05 and <0.0000005 respectively. (Description of node against node number was given in Table 62)

Fig. 162: Gene ontological enrichment analysis of topologically selected down-regulated genes based on biological process using BiNGO considering *Arabidopsis* as model organism. Hypergeometric test was conducted, considering p-value cut off ≤ 0.05. Size of the node was proportional to the number of gene (transcripts) present under a particular

nodal category. Node colour shades were according to the significance level where white represents no significant differences, green and blue colour shade represents significance level at p = 0.05 and <0.0000005 respectively. (Description of node against node number was given in Table 63)

Fig. 163: Kyoto Encyclopedia of Genes and Genomes (KEGG) classification of top differentially expressed (up-regulated) genes. The genes were enlisted at the top and the colour pattern (green shades) indicates the involvement of a particular gene in a particular KEGG pathway

Fig. 164: Kyoto Encyclopedia of Genes and Genomes (KEGG) classification of top differentially expressed (down-regulated) genes. The genes were enlisted at the top and the colour pattern (blue shades) indicates the involvement of a particular gene in a particular KEGG pathway

Fig. 165: Validation of key differentially expressed up-regulated genes using qRT-PCR analysis. The y-axis indicates relative quantification of the genes and the studied genes were indicated in the x-axis. Error bar indicates the value of standard deviation (±SD)

Fig. 166: Validation of key differentially expressed down-regulated genes using qRT-PCR analysis. The y-axis indicates relative quantification of the genes and the studied genes were indicated in the x-axis. Error bar indicates the value of standard deviation (±SD)

Fig. 167: Rearing pattern of silkworm larvae

Fig. 168: Average growth rate of larvae fed with fresh and preserved mulberry leaves

Fig. 169: Cocoon spinned by larvae after feeding with fresh mulberry leaves (**a**) and leaves preserved in distilled water (**b**), silver nitrate (**c**) and nanosilver (**d**) solution

Fig. 170: Effect of feeding S1 genotype of mulberry leaves, preserved with distilled water, nanosilver and silver nitrate on (**A**) growth index and (**B**) single cocoon weight. Silkworm larvae were fed with leaves preserved for 0D, 1D, 4D, 6D and 7D. The results were expressed as Mean ± SDEV, n= 3

Fig. 171: Effect of feeding S1 genotype of mulberry leaves, preserved with distilled water, nanosilver and silver nitrate on (**A**) single shell weight and (**B**) shell ratio. Silkworm larvae were fed with leaves preserved for 0D, 1D, 4D, 6D and 7D. The results were expressed as Mean ± SDEV, n= 3

Fig. 172: Effect of feeding S1 genotype of mulberry leaves, preserved with distilled water, nanosilver and silver nitrate on (**A**) effective rearing rate and (**B**) mortality rate. Silkworm

larvae were fed with leaves preserved for 0D, 1D, 4D, 6D and 7D. The results were expressed as Mean ± SDEV, n= 3

Fig. 173: (**a**) SDS gel portrait and (**b**) scanned image of silk gland protein obtained from larvae fed with (**1**) fresh leaves, (**2-4**) distilled water, nanosilver and silver nitrate preserved leaves respectively

Fig. 174: (**a-c**) Graphical representation depicting relative density of silk gland proteins obtained from SDS PAGE analysis. Numerical (1, 2, 3,...) at the top of graphical bars denotes band numbers

Fig. 175: (**a**) SDS gel portrait and (**b**) scanned image of haemolymph protein obtained from larvae fed with (**1**) fresh leaves, (**2-4**) distilled water, nanosilver and silver nitrate preserved leaves respectively

Fig. 176: (**a-c**) Graphical representation depicting relative density of haemolymph proteins obtained from SDS PAGE analysis. Numerical (1, 2, 3,...) at the top of graphical bars denotes band numbers

Fig. 177: (**a**) SDS gel portrait and (**b**) scanned image of stomach protein obtained from larvae fed with (**1**) fresh leaves, (**2-4**) distilled water, nanosilver and silver nitrate preserved leaves respectively

Fig. 178: (a-b) Graphical representation depicting relative density of stomach proteins obtained from SDS PAGE analysis. Numerical (1, 2, 3,...) at the top of graphical bars denotes band numbers

Fig. 179: (**a**) SDS gel portrait and (**b**) scanned image of fat body associated protein obtained from larvae fed with (**1**) fresh leaves, (**2-4**) distilled water, nanosilver and silver nitrate preserved leaves

Fig. 180: (a-b) Graphical representation depicting relative density of fat body associated proteins obtained from SDS PAGE analysis. Numerical (1, 2, 3,...) at the top of graphical bars denotes band numbers

Fig. 181: OHR-LCMS spectra of differentially expressed SDS band obtained from silk gland of larvae fed with nanosilver preserved leaves

Fig. 182: STRING analysis representing protein-protein interaction of differentially expressed silk gland proteins obtained from OHR-LCMS analysis

Fig. 183: On-gel (**a**) image and (**b**) scanned photograph showcasing NADPH oxidase activity inside silk gland of silkworm larvae fed with (**1**) fresh leaves, (**2-4**) leaves preserved in distilled water, nanosilver and silver nitrate solution respectively for 7 days

Fig. 184: (**a-b**) Graphical representation depicting relative density of NADPH oxidase activity inside silk gland of silkworm larvae fed with fresh leaves and 7 day preserved leaves in distilled water, nanosilver and silver nitrate solution respectively. Numerical (1, 2, 3,...) at the top of graphical bars denotes band numbers

Fig. 185: On-gel (**a**) image and (**b**) scanned photograph showcasing superoxide dismutase activity inside silk gland of silkworm larvae fed with (**1**) fresh leaves, (**2-4**) leaves preserved in distilled water, nanosilver and silver nitrate solution respectively for 7days

Fig. 186: Graphical representation depicting relative density of superoxide dismutase activity inside silk gland of silkworm larvae fed with fresh leaves and 7 day preserved leaves in distilled water, nanosilver and silver nitrate solution. Numerical (1, 2, 3,...) at the top of graphical bars denotes band numbers

Fig. 187: On-gel (**a**) image and (**b**) scanned photograph showcasing catalase activity inside silk gland of silkworm larvae fed with (**1**) fresh leaves, (**2-4**) leaves preserved in distilled water, nanosilver and silver nitrate solution respectively for 7days

Fig. 188: Graphical representation depicting relative density of catalase activity inside silk gland of silkworm larvae fed with fresh leaves and 7 day preserved leaves in distilled water, nanosilver and silver nitrate solution respectively. Numerical (1, 2, 3,...) at the top of graphical bars denotes band numbers

Fig. 189: Probable mechanism of action leading to post harvest shelf life extension in nanosilver preserved mulberry leaves

Fig. 190: Diagrammatic model of post harvest vascular blockage and its inhibition through nanosilver application

List of Appendices